*Journal of Engineering Research and Reports*

***Volume 25, Issue 2, Page 48-63, 2023; Article no.JERR.99171***
***ISSN: 2582-2926***

# Optimization of Brake Disc Profile Based on the Thermal Performance for Electric Vehicles

**Suvan S. Kudari [a] and A. Bharatish [a*]**

*[a] Department of Mechanical Engineering, RV College of Engineering, Bengaluru- 560059, India.*

***Authors' contributions***

*This work was carried out in collaboration between both authors. Both authors read and approved the final manuscript.*

***Article Information***

DOI: 10.9734/JERR/2023/v25i2879

**Open Peer Review History:**
This journal follows the Advanced Open Peer Review policy. Identity of the Reviewers, Editor(s) and additional Reviewers, peer review comments, different versions of the manuscript, comments of the editors, etc are available here: https://www.sdiarticle5.com/review-history/99171

***Original Research Article***

***Received: 05/03/2023***
***Accepted: 08/05/2023***
***Published: 16/05/2023***

## ABSTRACT

The brake disc market has reached the value of USD 20.9 billion in 2021 at a CAGR of 4.9% and it is expected to grow to USD 26.5 billion by 2026. However, the difficulties associated with the brake discs are significant rise in the temperature which results in, early wear, thermal cracks and brake fade leading to uneven braking and premature replacement. In this context many researchers have been studying the parameters like brake disc material and type of ventilation. The objective of the work was to study of the effect of ventilation types on thermal responses and optimize the brake disc profile for better thermal performances. Center of gravity and dynamic load transfer were calculated for two wheeler electric vehicle experimentally which was followed by computing the force required for braking process and heat flux on the brake disc analytically. Ventilation of type cross drilled holes (CD) was adopted in brake disc modelling, and was carried out in SOLIDWORKS 2022 and finite element model for the brake disc was created in ANSYS 17.2 with mesh size of 2 mm for lamellar graphite iron (LGI) with temperature dependent material properties. The transient thermal analysis for three braking cycles were carried out with the considerations such as: initial velocity of the vehicle of 96 km/h, ambient temperature of 22°C, conduction and convection modes of heat transfer and 5 s of deceleration and acceleration time. Transient thermal

**Corresponding author: Email: bharatisha@rvce.edu.in;*

analysis was carried out by applying the heat flux on the frictional surface of the brake disc. For the solid disc without ventilation, it was found that the maximum temperature at the end of first braking cycle (0 to 5 s) was 157.72°C, at end of second braking cycle (10 to 15 s) was 256.95°C and at the end of third braking cycle (20 to 25s) was 349.73°C. As the wear rate for lamellar graphite iron grows exponentially beyond 300°C, ventilations were provided on the brake disc to reduce the temperature on the disc. For the optimized brake disc with ventilation type VT-12, it was found that maximum temperature at the end of first braking cycle (0 to 5 s) was 139.43°C, at end of second braking cycle (10 to 15 s) was 222.68°C and at the end of third braking cycle (20 to 25s) was 299°C. The overall character of these shows a quick rise in temperature at the start of the process, followed by the achievement of the maximum value and, eventually there is a drop in temperature. In this research the future work can be carried out by implementing the noise, vibration and harness studies which would benefit the industry with better braking system.

*Keywords: Cross drill ventilation; heat flux; transient thermal analysis; Lamellar Graphite Iron (LGI).*

## 1. INTRODUCTION

Disc brakes are widely utilized on automobile and motorbike wheels in automotive applications and are usually made of cast iron disc that is fastened to the wheel hub. This is positioned between two pads that are supported in a calliper located on the stub shaft and are driven by pistons as shown in the Fig. 1. The opposing pistons and brake pads are pushed into frictional contact with the disc when the brake pedal is depressed, which is caused by hydraulically pressurized fluid being driven into the cylinders. This type of braking has the benefits of steady braking, simple design, easy ventilation, and balancing thrust loads. The braking action is proportional to the applied force because there is no self-energizing action. The net thrust load on the disc cancels as equal forces are applied to the pads on either side of it.

The brake system, which transforms mechanical energy into thermal energy [1,2] and distributes it through the discs and pads, is a crucial component of the locomotive safety system. The disc absorbs between 80 to 90 percent of the heat, which causes the brake disc's temperature to rise quickly and impairs braking performance [3].

It becomes very much important to consider the thermal behaviour of the brake disc and brake pad in the process of braking because rapid rise in the brake disc temperature reduces the braking performance and leads to thermal cracking, hot spots [3] brake fade and early wear [4]. Various parameters like brake disc profile, material, ventilation, etc. play important role in thermal behaviour. This led many researchers to do comprehensive study on thermal behaviour of the disc brake. Yang Ying et al. [5] investigated the effect of number of brake pads (14 and 18) and brake pad arrangements on temperature rise on brake disc resulted in the early stage of braking for ultra-deep mine hoist. Numerical simulations were carried out using direct coupling method. It was found that the increase in the number of brake pads does not improve the thermal performance but changing the brake pad arrangement has greater impact on thermal performance.

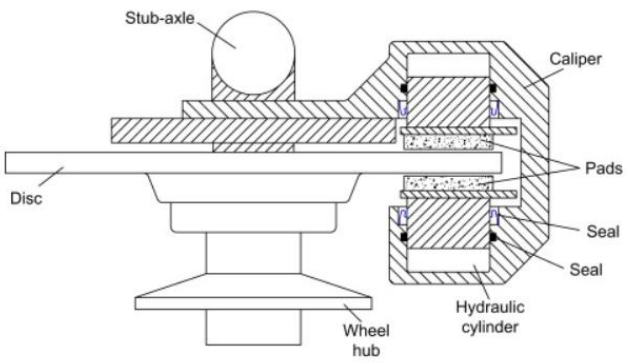


**Fig. 1. Automotive disc brake [21]**

Zhaojun Yang et al. [6] analysed the effect of pressing force (69, 84 and 99 kN) and friction coefficients between inboard pad and rotor (0.25, 0.35 and 0.45) and outboard pad and rotor (0.25, 0.35 and 0.45) on braking torque for ventilated air disc brake. Orthogonal experimental design L9 array was selected and dynamic analysis was carried out. It was observed that the braking torque is more sensitive to pressing force rather than friction coefficients. Whereas A.A. Yevtushenko et al. [7] investigated the disc brake of material cast iron and pad made of FMC11 at different values of contact pressure (0.59, 0.78, 1.18 and 1.47 MPa) and corresponding constant friction coefficients (0.672, 0.593, 0.507 and 0.448) and temperature dependent friction coefficients. Three dimensional FE contact model analysis is performed and resulting temperature fields, braking times and braking distances were found. Further A.A. Yevtushenko et al. [8] investigated the effect of temperature dependent friction coefficient on cast iron disc with FC-16L and FMC-11 pad materials at 1.47 MPa contact pressure. It was found that for friction pair of cast iron and FC-16L the maximum temperature attained was 112.3°C with 23.1% increase in friction coefficient whereas for cast iron and FMC-11 pair the maximum temperature attained was 97.1°C with 8.4% decrease in friction coefficient.

Lucival Malcher et al. [1] analysed steel SAE 1045 and stainless steel AISI 304 (brake disc material) for better heat dissipation. Amount of heat generated was calculated by braking power for 25 braking cycles. Transient thermal simulations were carried out where the heat flux was applied to the friction surface. It was found that steel SAE 1045 has better heat dissipating capacity than the stainless steel AISI 304. Whereas Tohid Mahmoudi et al. [4] analysed FG Al-A359/SiCp, aluminium, and ductile cast iron materials for functionally graded wheel mounted brake disc. Experimental tests and uncoupled thermo-mechanical analysis is performed. It was found that safety factor for FG material is higher than other materials considering the stress analysis. But maximum temperature in a braking cycle for FG material is 248.5°C and for aluminium and cast iron is 235.5°C.

Qifie Jian et al. [3] investigated heat pipe ventilated brake disc (HPVBD) for maximum heat dissipation and temperature uniformity. Experimental and simulation results were computed for repeated 15 braking and continuous downhill braking. It was found that, by introducing the heat pipes, temperature uniformity has increased by 36.675% and 21.435% and the heat dissipation has increased by 12.625% and 18.90% for repeated 15 braking and continuous downhill braking respectively. Further Qifie Jian et al. [9] investigated the transient temperature filed of automobile brake under hard braking in radial and circumferential direction. Experimental tests were performed on vehicle test bench along with finite element simulations. It was found that the temperature in friction zone was maximum in radial direction, the maximum temperature in the circumferential direction was same at all points but at different times. Pyung Hwang et al. [10] analysed the ventilated disc brake for temperature field and thermal stress during single brake cycle. Multi body model simulations with thermo-mechanical coupling boundary conditions were carried out along with experimental trials. It is found that the maximum contact pressure is occurred at mid circle of the contact region the mid stage of the braking cycle, and the maximum of 205.56° is occurred at the mid circle region. Ali Belhocine at al. [2] analysed the full brake disc and ventilated brake disc of cast iron (FG 15). Coupled thermo-mechanical and computational fluid dynamic simulations were carried out. It was found that the maximum temperature in full brake disc was 401.55°C and in ventilated disc brake was 345.44°C. Further the maximum thermal deformation and von misses stress on ventilated brake disc were found to be 284.55 μm and 495.56 MPa respectively.

A.A. Yevtushenko et al. [11] investigated the effect of temperature dependence on material properties such as coefficient of heat conduction and specific heat, keeping thermal diffusivity constant. Titanium pad is associated with different disc materials (steel disc, grey iron and aluminium alloy). Laplace transform and Newton-Rampson methods were used to find the numerical-analytical solutions and were compared with results obtained with constant thermo physical properties of disc and pad. It was found that at constant speed influence of thermo sensitive materials on temperature is increasing with increasing time of friction heating and at constant deceleration the influence of thermo sensitive materials on temperature was noticeable for steel-titanium system and least noticeable for grey iron-titanium system.

Faramarz Talati et al. [12] investigated the parameters like velocity of the vehicle, braking time, geometry and material of the brake disc.

Problem is solved using Green's approach. It was found that the wear particles were accumulated at the contact surface of disc and pad due to thermal resistance. In order to eliminate this, contrive slot was given on the pad.

D Meresse et al. [13] analysed the generated heat and temperature field using inverse heat conduction method. Heat flux examination is conducted for different braking conditions such as sliding speed and normal pressure on high speed Tribometer. Calculated heat fluxes were consistent with the friction power that is thermally dissipated. . Mesut Düzgün [14] analysed the four different types of ventilations (cross drilled, cross slotted and cross slotted with side groove) along with solid disc. Simulations and experimental results are compared for all the types of ventilation and it was found that maximum heat generation on the solid disc is reduced by 4% in cross drilled, where as 19% reduction in cross slotted and 24% reduction in cross slotted with groves. Piyush Chandra Verma [15] analysed the wear properties for different brake pad and disc material at higher temperature. It was found that grey cast iron would be suitable material for brake disc application due to good thermal conductivity and specific heat at higher temperature.

Vasilios Fourlakidis et al. [16] investigated the properties of lamellar graphite iron (LGI) and it was found that the specific heat of LGI at 773 K and 873 K are 590 J/kg-K and 700 J/kg-K respectively. Whereas Guang-hua Wang et al. [17] investigated the property of LGI at higher temperature and found out that the thermal conductivity at 300 K and 773 k were 58 W/m-K and 45 W/m-K respectively. You-Qun Zhao et al. [18] analysed the road friction coefficient in different road condition. It was found that road friction coefficient for dry asphalt, dry concrete, snow road and ice road were 0.95, 0.85, 0.18 and 0.3 respectively at 0.2 slip ratio. Aneta Bulí£ková [19] investigated the mesh quality in finite element method for different elements. For tetragonal element the acceptable ranges of aspect ratio is 1 to 1.3 and jacobian ratio 0.5 to 1 and for skewness is 0 to 0.5.

Review of the literature [1-20] revealed that the majority of the authors had considered SAE1045, AISI 304, etc materials for the brake disc by maintaining cross slotted ventilation type. Comparative studies about the various disc brake types and the variables that affect the thermal behavior of the disc are included in the literature. These studies allow us to take into account of factors, such as diameter of the cross ventilation, number of the hole for ventilation to optimize the thermal performance of the brake disc and cast iron as the material for the disc as the material shows good thermal conductivity at higher temperature.

## 2. MATERIALS AND METHODS

### 2.1 Material of the Brake Disc

The grey cast iron alloy is the most common type of cast iron used in braking discs. It has a pearlitic matrix with graphite particles. Due to the higher concentration of graphite in the microstructure of grey cast iron, which increases heat conductivity and permits lower temperatures in the area of friction [15]. In contrast to ductile iron, where spherical graphite particles are isolated from one another and therefore contribute very little to the thermal conductivity, which makes ductile iron have excellent strength and wear resistance comparable to other cast irons. Graphite flakes are interconnected and disposed in the form of plates, creating an easy path for fast heat dissipation [15]. Lamellar Graphite Iron (LGI) is considered for the brake disc material with the following properties shown in the Table 1 [16,17].

### 2.2 Locating Centre of Gravity Experimentally

During the process of deceleration the vehicle load will be partially shifted towards front wheel due to inertia. Due to this phenomenon braking force required in front wheel disc to stop the vehicle becomes more compared to rear wheel disc. Hence it becomes very much important to calculate location of centre of gravity and actual dynamic load transfer during braking. Fig. 2 shows the diagrammatic representation of two wheeler vehicle when front wheel is elevated while measuring centre of gravity.

The location centre of gravity is measured for two wheeler electric vehicle. The details are given in Table 2 whereas the Table 3 and Table 4 give the details of weight measurement of vehicle when kept horizontally and front wheel elevated respectively.

Where a is the location of centre of gravity from front wheel, h is the location of centre of gravity from ground, L (1.390 m) is wheel base, r (0.204 m) is radius of wheel and H (0.23m) is the height of elevation.

**Table 1. Material properties of lamellar graphite iron**

| Property | Value | At Temperature |
|---|---|---|
| **Density** | 7146 kg/m2 | |
| **Specific Heat** | 590 J/kg-K | 773 K |
| | 700 J/kg-K | 873 K |
| **Thermal Conductivity** | 58 W/m-K | 300 K |
| | 45 W/m-K | 773 K |

**Table 2. Location of centre of gravity**

| Condition | a (m) | h (m) |
|---|---|---|
| Vehicle | 0.831 | 0.376 |
| Vehicle and rider | 0.83 | 0.597 |
| Vehicle rider and Passenger | 0.92 | 0.862 |

**Table 3. Weight measurement of vehicle when kept horizontally**

| Weighing Condition | Front F or Rear R | Weight (kg) | Average (kg) |
|---|---|---|---|
| **Vehicle Weight (kg)** | F1 | 36.60 | 36.13 |
| | F2 | 36.80 | |
| | F3 | 35.00 | |
| | R1 | 53.25 | 54.32 |
| | R2 | 54.20 | |
| | R3 | 55.50 | |
| **Vehicle and Rider Weight (kg)** | F1 | 64.10 | 63.7 |
| | F2 | 64.30 | |
| | F3 | 62.70 | |
| | R1 | 93.90 | |
| | R2 | 93.80 | |
| | R3 | 95.70 | |
| **Vehicle, Rider and Passenger Weight (kg)** | F1 | 75.70 | 75.93 |
| | F2 | 75.90 | |
| | F3 | 76.20 | |
| | R1 | 151.60 | 152.67 |
| | R2 | 153.90 | |
| | R3 | 152.50 | |

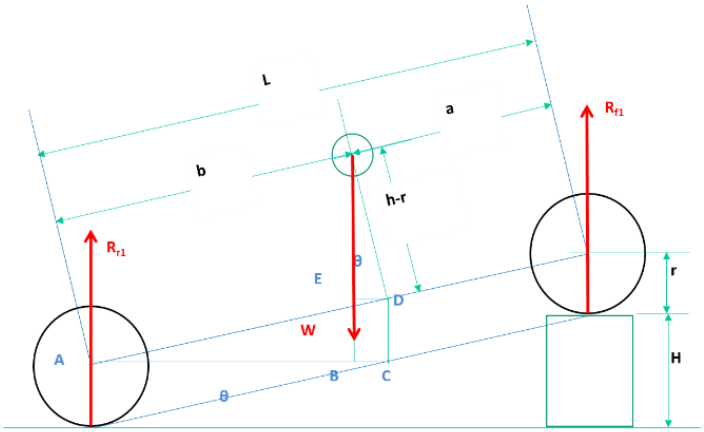


**Fig. 2. Locating centre of gravity**

**Table 4. Weight measurement of vehicle when front wheel is elevated**

| Weighing Condition | Front F | Weight (kg) | Average (kg) |
|---|---|---|---|
| **Vehicle Weight (kg)** | F1 | 34.20 | 34.25 |
| | F2 | 34.30 | |
| | F3 | 34.25 | |
| **Vehicle and Rider Weight (kg)** | F1 | 56.15 | 56.2 |
| | F2 | 55.75 | |
| | F3 | 56.70 | |
| **Vehicle, Rider and Passenger Weight (kg** | F1 | 57.50 | 57.77 |
| | F2 | 57.60 | |
| | F3 | 58.20 | |

## 2.3 Brake Disc Modelling

Brake disc is modelled in SOLIDWORKS 2022. Fig. 3 illustrated the details of modelling carried out in SOLIDWORKS 2022. Twelve ventilation model of different types are considered with cross drilled holes of different diameter. The effective frictional surface area lies between diameters 150 mm to 200 mm on the disc where disc pad comes in contact with disc. Ventilations are provided in the frictional surface area with holes of diameters 3.5 mm, 4 mm, and 4.5 mm. Three cross drill holes are provided in one group as shown in the detail A in Fig. 3. Three number of holes are drilled at pitch circle diameters 160 mm, 175 mm and 190 mm in one group.

Different types of ventilation on the disc is modelled and are shown in the Fig. 4 and the details of the same is provided in the Table 5.

## 2.4 Heat Flux Calculation

The brake system, which transforms mechanical energy into thermal energy [1,2] and distributes it through the discs and pads, is a crucial component of the locomotive safety system. The disc absorbs between 80 to 90 percent of the heat, which causes the brake disc's temperature to rise quickly. Hence the amount of heat entering the disc is calculated per mm2 of area (heat flux) on the frictional surface of the disc.

$$\text{Heat Flux} = \frac{mvv(1-d)(s)(\sigma)}{2tA} \quad (2.1)$$

Where the mass of the vehicle, rider and passenger, m is considered 228.6 kg. Initial velocity of the vehicle v is 96 kmph, the drag loss d is considered 0.27, dynamic load transfer to the front wheel s is considered 0.66 from Equation 2.4, heat partition ratio σ is considered 0.85 [3]. And surface area of the ventilated disc is calculated and tabulated in Table 6 along with calculated heat flux values.

$$W_f = F + W_d \quad (2.2)\ [20]$$

Where $W_f$ is dynamic front wheel load, F is the static front wheel load which is 75.93 kg from Table 4 and dynamic load factor $W_d$ is calculated from the Equation 2.3.

$$W_d = \frac{hWD}{lg} \quad (2.3)\ [20]$$

Where $W_d$ is dynamic load factor, h is 0.86 m, the center of gravity from the ground from Table 7 W is 228.6 kg, weight of the vehicle along with rider and passenger. l is 1.39 m, wheel base and g is acceleration due to gravity.

$$\text{Dynamic Load Transfer} = \frac{Wf}{W} \quad (2.4)\ [20]$$

## 2.5 Meshing and Boundary Condition

Ventilated brake discs were modelled in SOLIDWORKS 2022 and exported to ANSYS 17.2 for transient thermal analysis. Lamellar Grey Iron was considered as the disc material. Meshing was carried out using 4 node tetrahedron element and element size of 3 mm for all the twelve ventilation type of disc brakes. Fig. 5 shows the meshed model for ventilation type VT-1. The mesh quality is assessed in terms of aspect ratio, skewness and jacobian ratio [14]. The mesh quality details are shown in the Table 7.

Transient thermal analysis is considered for 3 braking cycles for 30 s with deceleration and acceleration of 5 m/s2. Fig. 6 shows the details of velocity vs. time plot over the period of 3 braking cycles.

**Table 5. Details of ventilation types**

| Ventilation Type | Hole Diameter (mm) | No. of Holes in a Group | Number of Groups | Total Number of Holes | Ventilation Details |
|---|---|---|---|---|---|
| VT-1 | 3.5 | 3 | 10 | 30 | Cross drill holes of diameter 3.5 mm (30 no. of holes) |
| VT-2 | 4 | 3 | 10 | 30 | Cross drill holes of diameter 4 mm (30 no. of holes) |
| VT-3 | 4.5 | 3 | 10 | 30 | Cross drill holes of diameter 4.5 mm (30 no. of holes) |
| VT-4 | 3.5 | 3 | 15 | 45 | Cross drill holes of diameter 3.5 mm (45 no. of holes) |
| VT-5 | 4 | 3 | 15 | 45 | Cross drill holes of diameter 4 mm (45 no. of holes) |
| VT-6 | 4.5 | 3 | 15 | 45 | Cross drill holes of diameter 4.5 mm (45 no. of holes) |
| VT-7 | 3.5 | 3 | 20 | 60 | Cross drill holes of diameter 3.5 mm (60 no. of holes) |
| VT-8 | 4 | 3 | 20 | 60 | Cross drill holes of diameter 4 mm (60 no. of holes) |
| VT-9 | 4.5 | 3 | 20 | 60 | Cross drill holes of diameter 4.5 mm (60 no. of holes) |
| VT-10 | 3.5 | 3 | 25 | 75 | Cross drill holes of diameter 3.5 mm (75 no. of holes) |
| VT-11 | 4 | 3 | 25 | 75 | Cross drill holes of diameter 4 mm (75 no. of holes) |
| VT-12 | 4.5 | 3 | 25 | 75 | Cross drill holes of diameter 4.5 mm (75 no. of holes) |

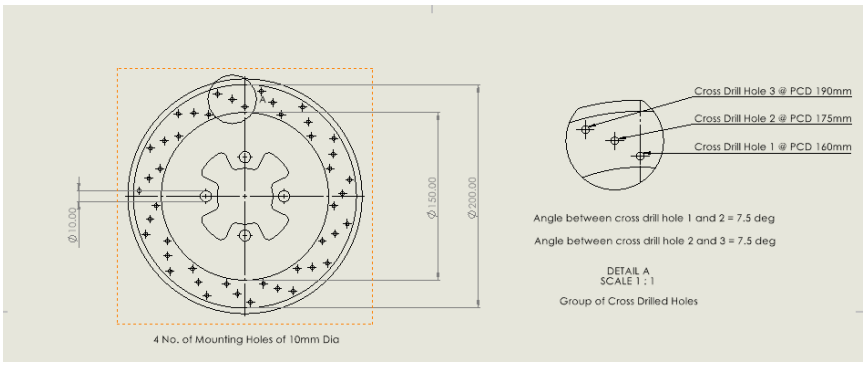


**Fig. 3. Brake disc modelling**

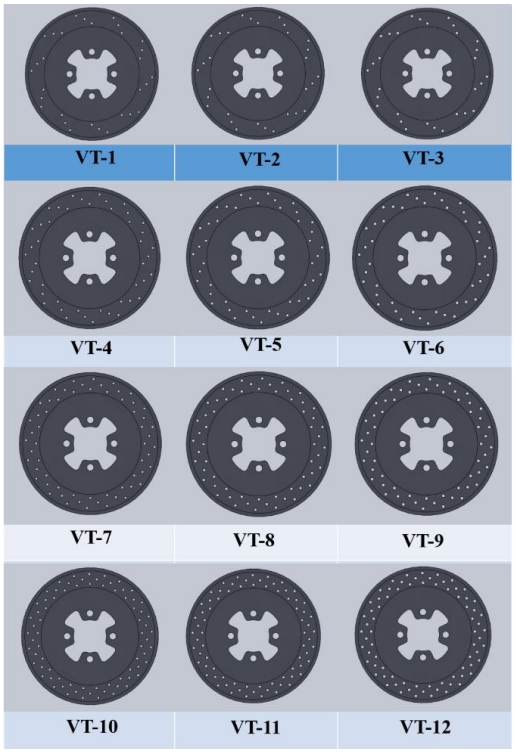


**Fig. 4. CAD model of ventilated discs**

**Table 6. Details of heat flux and surface area for different ventilation types**

| Sl. No. | Ventilation Type | Surface Area (mm2) | Heat Flux (w/mm2) |
|---|---|---|---|
| 1 | VT-1 | 28561.01 | 0.2991 |
| 2 | VT-2 | 28619.92 | 0.2985 |
| 3 | VT-3 | 28655.26 | 0.2981 |
| 4 | VT-4 | 29097.05 | 0.2936 |
| 5 | VT-5 | 29185.4 | 0.2927 |
| 6 | VT-6 | 29238.42 | 0.2921 |
| 7 | VT-7 | 29633.08 | 0.2882 |
| 8 | VT-8 | 29750.89 | 0.2871 |
| 9 | VT-9 | 29821.22 | 0.2864 |
| 10 | VT-10 | 30169.12 | 0.2831 |
| 11 | VT-11 | 30316.38 | 0.2818 |
| 12 | VT-12 | 30404.73 | 0.2809 |

**Table 7. Mesh details**

| Sl. No. | Ventilation Type | Number of Nodes | Number of elements | Aspect Ratio | Skewness | Jacobian Ratio |
|---|---|---|---|---|---|---|
| 1 | VT-1 | 261575 | 168341 | 1.894 | 0.24825 | 0.96444 |
| 2 | VT-2 | 85784 | 50559 | 1.9068 | 0.24226 | 0.8369 |
| 3 | VT-3 | 86812 | 51041 | 1.9267 | 0.24918 | 0.76711 |
| 4 | VT-4 | 262825 | 168107 | 1.9044 | 0.25298 | 0.90223 |
| 5 | VT-5 | 82623 | 48984 | 1.8825 | 0.23442 | 0.955 |
| 6 | VT-6 | 83109 | 49002 | 1.8748 | 0.23215 | 0.95846 |
| 7 | VT-7 | 83755 | 49276 | 1.8932 | 0.23965 | 0.91852 |
| 8 | VT-8 | 83874 | 48965 | 1.8895 | 0.23914 | 0.91694 |
| 9 | VT-9 | 82727 | 48973 | 1.8767 | 0.23281 | 0.95498 |
| 10 | VT-10 | 82624 | 48702 | 1.8768 | 0.23195 | 0.9555 |
| 11 | VT-11 | 260829 | 166752 | 1.9035 | 0.25333 | 0.99595 |
| 12 | VT-12 | 83357 | 48754 | 1.8871 | 0.23726 | 0.80726 |
| 13 | Without Ventilation | 82038 | 49111 | 1.8762 | 0.23184 | 0.975 |

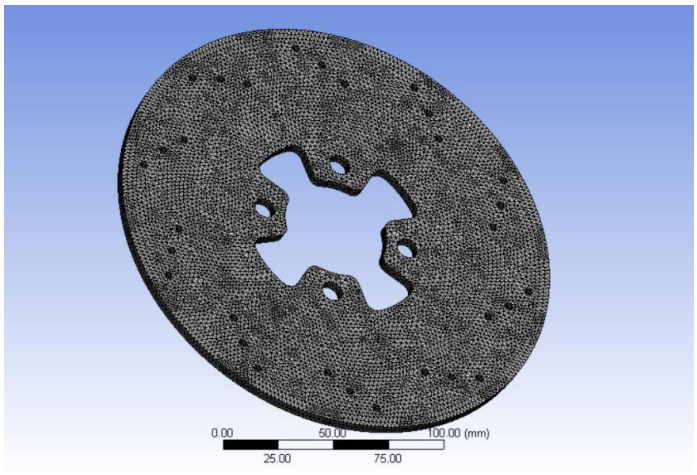


**Fig. 5. Finite element model for VT-1 ventilation**

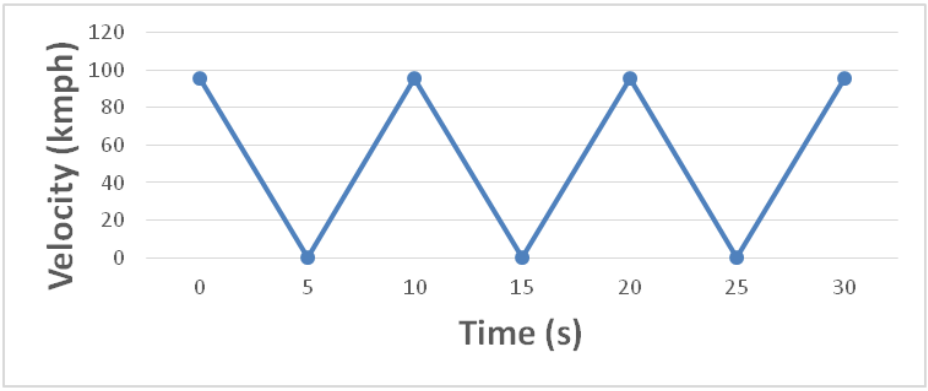


**Fig. 6. Velocity vs. Time plot**

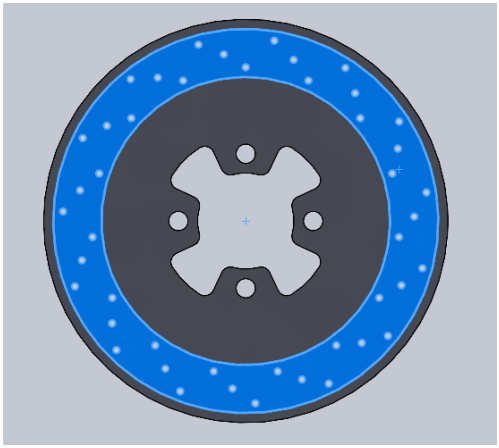

**Fig. 7. Heat flux on frictional surface**

According the details of braking cycles the computed heat flux is applied on the frictional surface as shown in Fig. 7 for the range of 0-5 s, 10-15 s and 20-25 s. And the average convection of 10 W/m$^2$-K with ambient temperature of 22°C is applied for the entire body. Lamellar Graphite Iron (LGI) is considered as the disc material for transient thermal analysis with temperature dependent properties (density, specific heat and thermal conductivity) [16,17].

## 3. RESULTS AND DISCUSSION

### 3.1 Results

Transient thermal analysis was carried out by applying the calculated heat flux is applied on the frictional surface of the brake disc. The temperature distribution on the disc surface at the end of 30 s as shown in the Fig. 8 for all the types of ventilations. Fig. 9 shows the temperature distribution for the disc without ventilation. Temperature versus time results are plotted for disc with all ventilation types as shown in the Fig. 10 and disc without ventilation as shown in the Fig. 11.

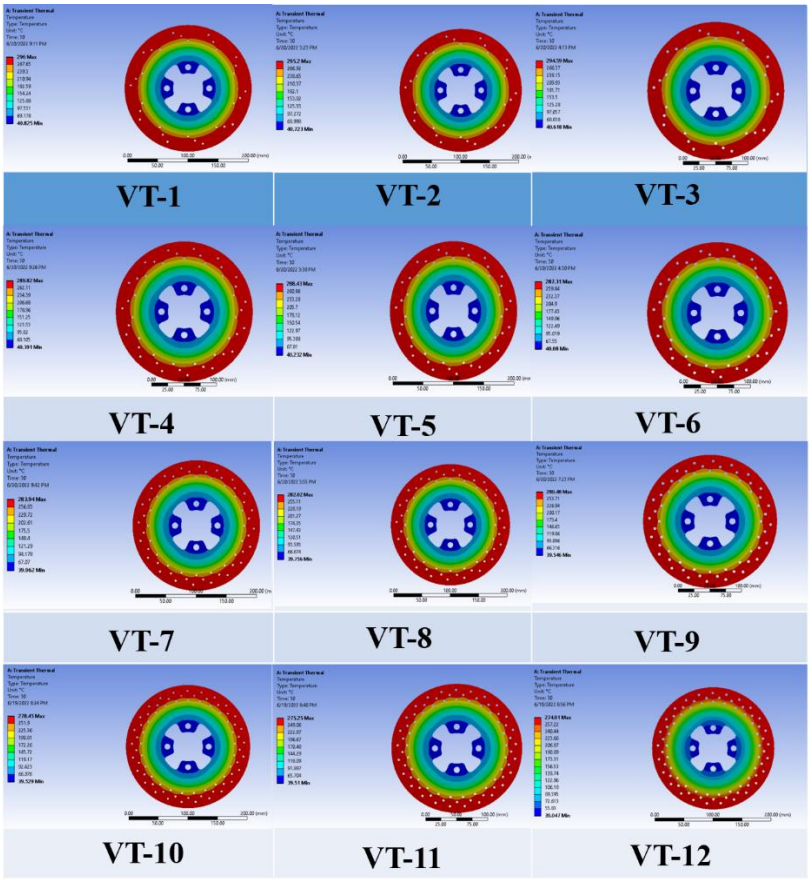


**Fig. 8. Simulation results for disc with different ventilation**

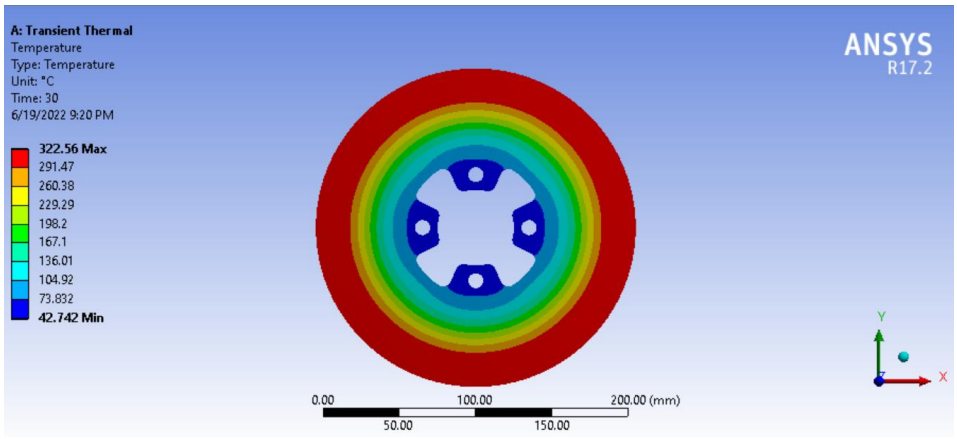


**Fig. 9. Simulation results for disc without ventilation**

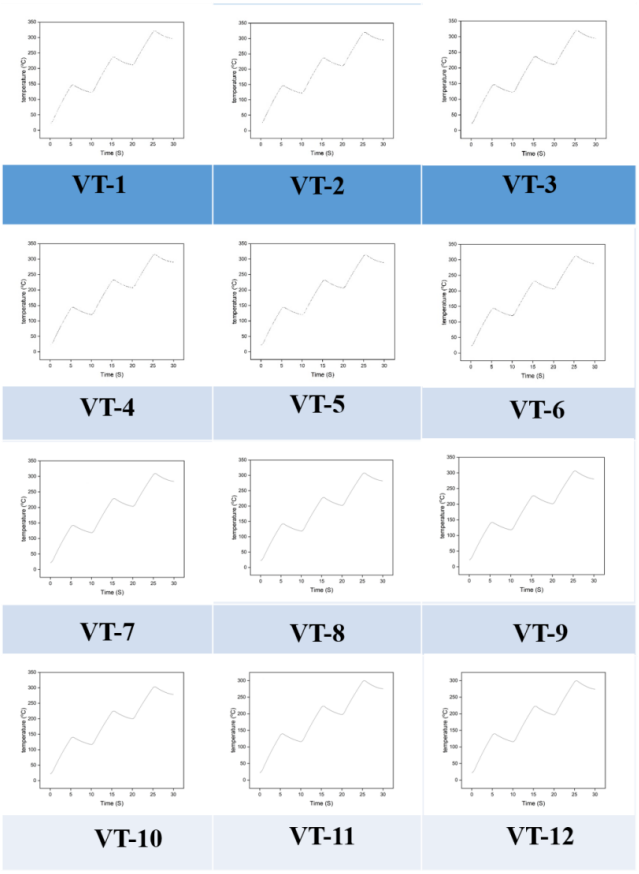


**Fig. 10. Time vs. Temp plot for ventilated disc**

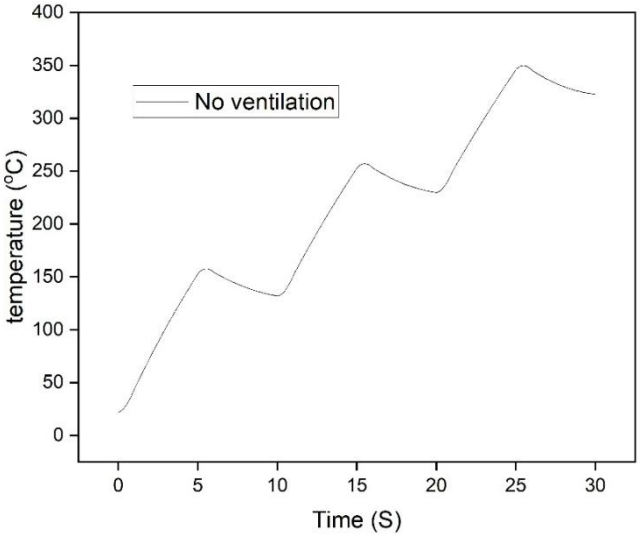


**Fig. 11. Time vs. Temp plot for non- ventilated disc**

## 3.2 Discussion

It is observed that the maximum temperature for disc without ventilation after 3rd braking cycle is 349.9 °C, which is considered as the maximum wear rate zone as the wear rate increases exponentially after 300°C [15]. Hence ventilation is provided on the disc to reduce the temperature on the disc. Basically ventilation increases the surface area of the disc by which the heat flux

reduces as they are inversely related. As the heat flux is directly proportional to the temperature rise on disc, Ventilation is provided with parameters like hole diameter and number of cross drilled holes to increase the convective heat transfer area there by reducing the heat flux entering the disc. The overall character of these shows a quick rise in temperature at the start of the process, followed by the achievement of the maximum value and, eventually there is a drop in temperature. The phenomenon naturally occurs pertaining to the connection between the thermal load and its concomitant conduction-mediated absorption and convection, although it doesn't significantly affect regular single-phase flow circumstances for braking. Referring to the Table 6 the graph is plotted for ventilation type and surface area as shown in the Fig. 12 and plot for ventilation type and heat flux can be seen in the Fig. 13.

For the ventilation types of VT-1, VT-2 and VT-3 reduction in the maximum temperature are 8.28%, 8.39% and 8.53% respectively compared to disc without ventilation. By increasing the number of holes i.e. for ventilation types VT-4, VT-5 type and VT-6 the reduction in the maximum temperature are 10.01%, 10.37% and 10.63% respectively compared to disc without ventilation. Further increasing in the number of holes i.e. for ventilations types VT-7, VT-8 and VT-9 the reduction in the maximum temperature are 11.65%, 12.13% and 12.46% respectively compared to disc without ventilation. Finally for ventilations types VT-10, VT-11 and VT-12 the reduction in the maximum temperature are 13.25%, 14.26% and 14.49% respectively. Fig. 14 shows the plot percentage reduction in maximum temperature for different ventilations and Table 8 shows the temperature distribution on the disc surface during various braking cycles.

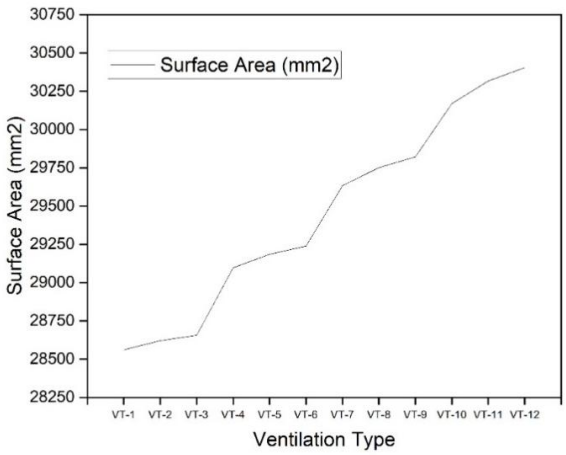


**Fig. 12. Ventilation type vs. surface area**

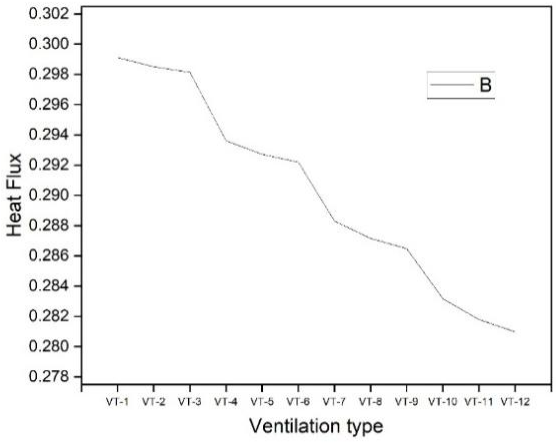


**Fig. 13. Ventilation type vs. heat flux**

**Table 8. Temperature distribution at different braking cycle**

| Sl. No. | Ventilation Type | Temperature °C | | | | | |
|---|---|---|---|---|---|---|---|
| | | 1st Braking Cycle | | 2nd Braking Cycle | | 3rd Braking Cycle | |
| | | 5 s | 10 s | 15 s | 20 s | 25 s | 30 s |
| 1 | VT-1 | 146.59 | 122.51 | 236.88 | 211.59 | 320.74 | 296 |
| 2 | VT-2 | 146.45 | 122.32 | 236.44 | 211.1 | 320.36 | 295.2 |
| 3 | VT-3 | 146.45 | 122.2 | 236.23 | 210.74 | 319.88 | 294.59 |
| 4 | VT-4 | 144.26 | 120.43 | 232.49 | 207.34 | 314.7 | 289.82 |
| 5 | VT-5 | 144 | 120.07 | 231.76 | 206.46 | 313.45 | 288.43 |
| 6 | VT-6 | 143.92 | 119.84 | 231.26 | 205.75 | 312.52 | 287.31 |
| 7 | VT-7 | 142.32 | 118.62 | 228.65 | 203.26 | 308.94 | 283.94 |
| 8 | VT-8 | 142.02 | 118.17 | 227.74 | 202 | 307.28 | 282.02 |
| 9 | VT-9 | 141.98 | 117.91 | 227.17 | 200.99 | 306.13 | 280.48 |
| 10 | VT-10 | 140.23 | 116.73 | 224.79 | 199.58 | 303.36 | 278.45 |
| 11 | VT-11 | 139.55 | 115.89 | 222.8 | 197.55 | 299.83 | 275.25 |
| 12 | VT-12 | 139.43 | 115.7 | 222.68 | 196.71 | 299 | 274 |
| 13 | Without Ventilation | 157.72 | 131.84 | 256.95 | 229.7 | 349.73 | 322.56 |

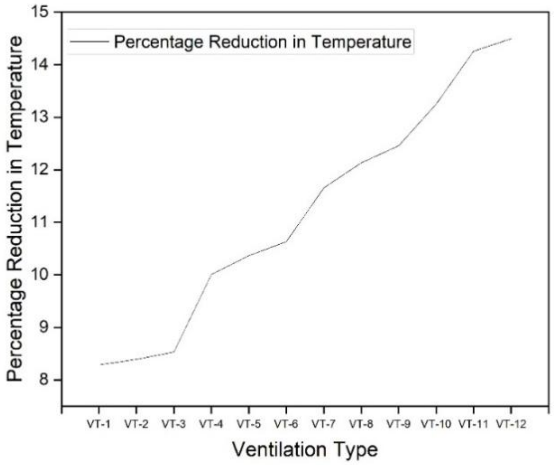


**Fig. 14. Ventilation type vs. percentage reduction in the temperature**

## 4. CONCLUSION

In this project the effect of ventilation is studied on the brake disc for three braking cycles in the two wheeler vehicle. Modelling of brake disc is carried out in SOLIDWORKS 2022 and transient thermal simulations are carried out in ANSYS 17.2. Lamellar Graphite Iron (LGI) is consider for the brake disc material.

- The simulations were carried out for 30 s and for 3 braking cycles with maximum speed of vehicle being 96 km/h. Acceleration and deceleration times were considered as 5 s.
- The temperature field plots shows that the maximum temperature occurs at the surface of the friction.
- The rise in the temperature in non-ventilated brake disc for three braking cycles leads to cause maximum wear rate on the disc as the temperature reaches 349°C.
- Simulations were carried out by providing the ventilations on the disc which increases the surface area and reduces the heat flux on the disc resulting in the decrease in the temperature
- For the ventilation type VT-12 the maximum temperature was about 299°C, which is 50°C lesser than the temperature observed in brake disc without ventilation.

## COMPETING INTERESTS

Authors have declared that no competing interests exist.

## REFERENCES

1. Pasqual, Gustavo Varejão Ferreira, and Lucival Malcher. ENC-2020-0644 Thermal analysis of brake discs for BAJA SAE vehicle.
2. Belhocine Ali, Mostefa Bouchetara. Thermal–mechanical coupled analysis of a brake disk rotor. Heat and Mass Transfer. 2013;49.8:1167-1179.
3. Jian, Qifei, Li Wang, Yan Shui. Thermal analysis of ventilated brake disc based on heat transfer enhancement of heat pipe. International Journal of Thermal Sciences. 2020;155:106356.
4. Mahmoudi Tohid, et al. Thermo-mechanical analysis of functionally graded wheel-mounted brake disk. Journal of Mechanical Science and Technology. 2015;29.10:4197-4204.
5. Yang Ying, Xuelong Ye. Research and optimization on thermal performance of brake disc for ultra deep mine hoist." 2018 10th International Conference on Measuring Technology and Mechatronics Automation (ICMTMA). IEEE; 2018.
6. Yang Zhaojun, et al. Dynamic analysis of disc brake and impact law of related parameters on braking torque. The 2010 IEEE International Conference on Information and Automation. IEEE; 2010.
7. Yevtushenko AA, Grzes P. Mutual influence of the sliding velocity and temperature in frictional heating of the thermally nonlinear disc brake. International Journal of Thermal Sciences. 2016;102:254-262.

8. Yevtushenko AA, Adamowicz A, Grzes P. Three-dimensional FE model for the calculation of temperature of a disc brake at temperature-dependent coefficients of friction. International Communications in Heat and Mass Transfer. 2013;42:18-24.
9. Jian Qifei, Yan Shui. Numerical and experimental analysis of transient temperature field of ventilated disc brake under the condition of hard braking. International Journal of Thermal Sciences. 2017;122:115-123.
10. Hwang Pyung, Xuan Wu. Investigation of temperature and thermal stress in ventilated disc brake based on 3D thermo-mechanical coupling model. Journal of mechanical science and technology. 2010; 24.1:81-84.
11. Yevtushenko AA, Kuciej M, Och E. Influence of thermal sensitivity of the pad and disk materials on the temperature during braking. International Communications in Heat and Mass Transfer. 2014;55:84-92.
12. Talati Faramarz, Salman Jalalifar. Analysis of heat conduction in a disk brake system. Heat and Mass Transfer. 2009;45.8: 1047-1059.
13. Méresse Damien, et al. Experimental disc heat flux identification on a reduced scale braking system using the inverse heat conduction method. Applied Thermal Engineering. 2012;48:202-210.
14. Duzgun, Mesut. Investigation of thermo-structural behaviors of different ventilation applications on brake discs. Journal of Mechanical Science and Technology. 2012;26.1:235-240.
15. Verma, Piyush Chandra. Automotive brake materials: Characterization of wear products and relevant mechanisms at high temperature. Diss. University of Trento; 2016.
16. Fourlakidis Vasilios, Ilia Belov, Attila Diószegi. Strength prediction for pearlitic lamellar graphite iron: Model validation. Metals. 2018;8.9:684.
17. Wang, Guang-hua, Yan-xiang Li. Thermal conductivity of cast iron-A review. China Foundry. 2020;17.2:85-95.
18. You-Qun Zhao, Hai-Qing Li, Fen Lin, Jian Wang and Xue-Wu Ji. Estimation of road friction coefficient in different road conditions based on vehicle braking dynamics. Chinese Journal of Mechanical Engineering. 2017;30.4: 982-990.
19. Aneta Bulíčková. Quality evaluation of finite element models with applications on concrete structures. MS thesis. České vysoké učení technické v Praze. Vypočetní a informační centrum; 2020.
20. Schramm Dieter, Manfred Hiller, Roberto Bardini. Vehicle dynamics. Modeling and Simulation. Berlin, Heidelberg. 2014; 151.
21. Chen F. Automotive disk brake squeal: an overview. International Journal of Vehicle Design. 2009;51(1-2):39-72.



*Peer-review history:*
*The peer review history for this paper can be accessed here:*
*https://www.sdiarticle5.com/review-history/99171*